Fuel Processing Technology 159 (2017) 160–167

Contents lists available at ScienceDirect

Fuel Processing Technology

journal homepage: www.elsevier.com/locate/fuproc

Research article

In-situ catalytic pyrolysis of peanut shells using modified natural zeolite

L.I. Gurevich Messina [a,b], P.R. Bonelli [a,b], A.L. Cukierman [a,b,c,*]

[a] Programa de Investigación y Desarrollo de Fuentes Alternativas de Materias Primas y Energía—PINMATE, Departamento de Industrias, Facultad de Ciencias Exactas y Naturales, Universidad de Buenos Aires, Intendente Güiraldes 2620, Ciudad Universitaria, C1428BGA Buenos Aires, Argentina
[b] Consejo Nacional de Investigaciones Científicas y Técnicas (CONICET), Godoy Cruz 2290, C1425FQB Buenos Aires, Argentina
[c] Cátedra de Tecnología Farmacéutica II, Departamento de Tecnología Farmacéutica, Facultad de Farmacia y Bioquímica, Universidad de Buenos Aires, Junín 956, C1113AAD Buenos Aires, Argentina

ARTICLE INFO

Article history:
Received 21 June 2016
Received in revised form 9 January 2017
Accepted 18 January 2017
Available online xxxx

Keywords:
Catalytic pyrolysis
Peanut shells
Clinoptilolite
Bio-oil quality improvement

ABSTRACT

In-situ catalytic pyrolysis of peanut (*Arachis hypogaea*) shells was investigated employing modified clinoptilolite. Likewise, conventional pyrolysis of the shells was explored to quantify the deoxygenation degree of bio-oil. Two solid catalysts obtained from natural clinoptilolite were used: one which retained most of the native cations and another one subjected to ion exchange treatment to develop Brønsted acid sites. These catalysts were characterized using different techniques, such as scanning electron microscopy with X-ray microanalysis, Fourier transform infrared spectroscopy by pyridine adsorption, and nitrogen sorptometry. Assays in a bench scale installation based on a fixed bed reactor were conducted at 500 °C and the yields of the three kinds of pyrolysis products (bio-oil, bio-char and gases) were determined. Likewise, the composition and other physical properties of the bio-oil and gases were investigated. Both catalysts led to reduce the oxygen content of the bio-oil, improving its high heating value. On the other hand, catalytic pyrolysis promoted a slight reduction in bio-oil production at expenses of an increase in gases generation. The catalyst subjected to ion exchange performed better than the native form as less water was generated in the catalytic cracking.

1. Introduction

Argentina is one of the largest producing countries of peanut (*Arachis hypogaea*) with an estimated annual production of over 1 Mt [1]. Industrial processing of peanut generates a large amount of shells, accounting for approximately one fourth of the annual production of the legume. This waste is normally burned, releasing into the atmosphere toxic gases, such as dioxins [2–4]. Waste burial, which is also employed to dispose the hulls, could lead to changes in soil pH and may result in groundwater pollution. Bioenergy production from biomass resources would minimize these practices, contributing at the same time to generate green energy [5–8].

As the peanut shells are rich in lignin, biochemical processes, such as anaerobic digestion or alcoholic fermentation, are not appealing because of their lower organic matter degradation capacity. On the other hand, thermochemical processes such as gasification or pyrolysis, could decompose lignin and also attain higher reaction rates [9]. Despite being a more mature technology, gasification produces gases with a low energy density and which are expensive to transport and storage. By contrast, biomass pyrolysis generates a high energy density liquid fuel, known as bio-oil, which could be used as substitute of fuel-oil [10]. This biofuel has been tested in boilers and gas turbines, reaching a high degree of combustion efficiency [11].

However, bio-oil shows some disadvantages mainly due to its high oxygen content. The oxygenated compounds present in the liquid lead to a high chemical polarity, which reduces its miscibility with conventional hydrocarbon fuels. Furthermore, most of the oxygen is in the form of reactive groups (hydroxyl and carboxyl groups) that might react among them, lowering the bio-oil stability. In addition, the high oxygen content brings about a low heating value of the bio-oils [8,9,12,13].

Among the different alternatives to improve the bio-oil quality by lowering its oxygen content, zeolite cracking is one of the most promising options [14,15]. By means of this process, bio-oil deoxygenation is accomplished through dehydration, decarbonylation, decarboxylation, and cracking. The acid nature of zeolites is the main motive of their catalytic activity as it seems to promote the rupture of C—C and C—O bonds through the acid sites [16]. The zeolite based catalysts could be used to improve the bio-oil in different ways. The bio-oil upgrading might be carried out in a different reactor than the one used to carry out the pyrolysis, allowing to make react the vapours or the bio-oil with the catalysts. On the other hand, the same reactor where the pyrolysis is performed could be employed to accomplish catalysis. This scheme is known as *in-situ* catalytic pyrolysis [17].

* Corresponding author at: Programa de Investigación y Desarrollo de Fuentes Alternativas de Materias Primas y Energía—PINMATE, Departamento de Industrias, Facultad de Ciencias Exactas y Naturales, Universidad de Buenos Aires, Intendente Güiraldes 2620, Ciudad Universitaria, C1428BGA Buenos Aires, Argentina.
E-mail address: analea@di.fcen.uba.ar (A.L. Cukierman).

http://dx.doi.org/10.1016/j.fuproc.2017.01.032
0378-3820/

Synthetic zeolites, such as ZSM-5, mordenite and faujasite, are usually employed to develop the catalysts [15,18]. Nevertheless, the cracking could also be performed employing natural zeolites, therefore, reducing the cost of the process. Clinoptilolite, being the most abundant zeolite in the earth crust, is an attractive option to develop cheap catalysts [19]. However, only few works on the subject have explored zeolite cracking with clinoptilolite as a way to improve pyrolysis products. Pütun et al. [20] compared the catalytic pyrolysis of residues of olive oil production using ZSM-5 and clinoptilolite. They concluded that, although the synthetic zeolite was more effective to deoxygenate the bio-oil than the clinoptilolite, less coke was produced employing the latter as catalyst. Moreover, Rajić et al. [21] explored the synergy between metal oxides and clinoptilolite in lignin pyrolysis for phenol production. In later works, they compared the performance of phenol production between the modified clinoptilolite and the modified ZSM-5 [22,23], finding that phenol production depended mainly on the metal cations in the zeolite and not on the type of acid sites. Nevertheless, the quantity and type of acid sites (Lewis and Brønsted sites) has been reported to exert a strong influence on the cracking process [24]. However, to the best of our knowledge, there are no works in the literature devoted to examine exhaustively the influence of the different acid sites of clinoptilolite on the pyrolysis products.

Within this context, this work comparatively studies the conventional pyrolysis of peanut shells and catalytic pyrolysis of this lignocellulosic biomass using two catalysts developed from clinoptilolite. One of the catalysts retained most of the cations present in the natural clinoptilolite while the other was subjected to an ion exchange treatment in order to protonate it and increase Brønsted acid sites concentration. Pyrolysis of the shells was performed employing a fixed bed reactor at pre-established conditions. Yields of the different pyrolysis products were obtained. The gases and bio-oils generated were also characterized.

2. Materials and methods

2.1. Peanut shells

Commercial peanut (*Arachis hypogaea*) shells, abbreviated as PS, were cleaned, milled, and screen-sieved in order to obtain samples of different particle diameters. The fraction ranging from 250 μm to 500 μm was selected for the fixed bed reactor experiments, while that of particle diameter between 44 and 74 μm was used for thermogravimetric studies. The elemental composition of the biomass samples was determined using an automatic elemental analyzer (Carlo Erba model EA 1108) and the content of main biopolymers of the shells was estimated by Van Soest analysis. The elemental content [wt%, dry and ash-free basis] of the hulls was C: 49.6; H: 6.5; N: 1.8; O: 42.1. Moreover, the biopolymer composition [wt%, dry and ash-free basis] was the following: lignin: 30.9; cellulose: 54.6; hemicellulose: 14.5.

2.2. Natural zeolite and catalyst development

Natural clinoptilolite, shortened CL, provided by Minera CMA was employed. It was milled and sieved. The aforementioned particle sizes (44–74 μm and 250–500 μm) were employed.

An alkaline catalyst (Z1) was obtained by calcinating the clinoptilolite at 500 °C for 24 h. On the other hand, in order to obtain a protonated catalyst (Z2), the zeolite was submitted to ion exchange with NH_4Cl. This treatment was accomplished using 20 mL of a 0.5 M NH_4Cl solution per gram of clinoptilolite. The ion exchange was carried out in a beaker without agitation and at ambient temperature by 8 h. Afterwards the material was filtered and washed until absence of Cl^-, which was verified with a $AgNO_3$ solution. Finally, the material was calcinated for 24 h in order to decompose NH_4^+ into H^+ [25]. Before the catalytic experiments, the catalysts were activated heating the samples at 400 °C for 1 h.

2.3. Zeolite and catalyst characterization

The clinoptilolite and the catalysts phases were identified by means of X-ray diffraction (XRD) using a Siemens D5000 diffractometer with Cu Kα radiation (λ = 1.54056 Å). The scanning angle was in the range 5–60° of 2θ with a step size of 0.05° and a scanning speed of 2.0 s $step^{-1}$.

In addition, both the native zeolite and the catalysts were analyzed by scanning electronic microscopy (SEM) in a Zeiss Supra 40 coupled with an Oxford-Instrument energy dispersive X-ray (EDS) spectrophotometer. Prior to the analysis, the samples were placed on an aluminum holder, supported on conductive carbon tape, dried under vacuum, and sputter coated with Au-Pd.

pH of the samples was measured suspending 1 g of each one in 20 mL of distillated water and letting boil for about an hour. Then, the solution was cooled to room temperature and the pH value was assessed using a portable Orion 290A pH-meter.

Concentrations of Brønsted and Lewis acid sites were quantified by pyridine adsorption coupled to FT-IR spectroscopy. The concentration (C) was calculated as:

$$C = (A \cdot s_d)/(\varepsilon \cdot W_d) \quad (1)$$

The integrated absorbance (A) of peaks corresponding to Brønsted (1545 cm^{-1}) and Lewis (1445 cm^{-1}) sites was used. W_d and s_d represent, respectively, the weight and the area of the sample disk which was mounted on the spectrophotometer. The molar extinction coefficients (ε) measured by Emeis [26] were employed: 2.22 cm μmol^{-1} for Lewis sites, and 1.67 cm μmol^{-1} for Brønsted sites. The strength of the different acid sites was determined quantifying the adsorbed pyridine after desorption at different temperatures (100 °C, 200 °C, 300 °C, and 400 °C).

Moreover, N_2 adsorption isotherms of the materials at −196 °C were determined using an automatic Micromeritics ASAP-2020 HV volumetric sorption analyzer. Before the analysis, the samples were outgassed at 120 °C for 2 h. Textural properties were assessed from the isotherms, according to conventional procedures depicted in detail in previous studies [27]. The Brunauer-Emmett-Teller (BET) surface area (S_{BET}) was determined by the standard BET procedure and total pore volumes (V_t) were estimated from the amount of nitrogen adsorbed at the relative pressure of 0.95 ($p/p_0 = 0.95$). Mean pore radius (R_m) was calculated as

$$R_m = 2\,V_t/S_{BET} \quad (2)$$

2.4. Thermogravimetric assays

Measurements of the pyrolysis behavior of the peanut shells, individually and in the presence of each catalyst (biomass to catalyst ratio of 2:1), were carried out in a simultaneous thermal analyzer (TG-DSC/DTA TA Instruments SDT Q600). The samples were thermally treated under a constant flow of N_2 (100 mL min^{-1}) from ambient temperature up to 500 °C. Experiments were performed for samples' masses of 10 mg, fractions of 44–74 μm particle diameter, and heating rate of 10 °C min^{-1}. For these conditions, negligible diffusional effects were thoroughly verified from preliminary experiments.

2.5. Conventional and in-situ catalytic pyrolysis assays

In order to obtain the pyrolysis products and determine their yields, pyrolysis experiments were carried out in a bench-scale fixed bed reactor (2.5 cm I.D., 110 cm total length) made of AISI 316 stainless steel (Fig. 1). Peanut shells, individually and mixed with each one of the catalysts (biomass to catalyst ratio of 2:1), were first placed at room temperature in a sample carrier located in a zone above the reactor, that

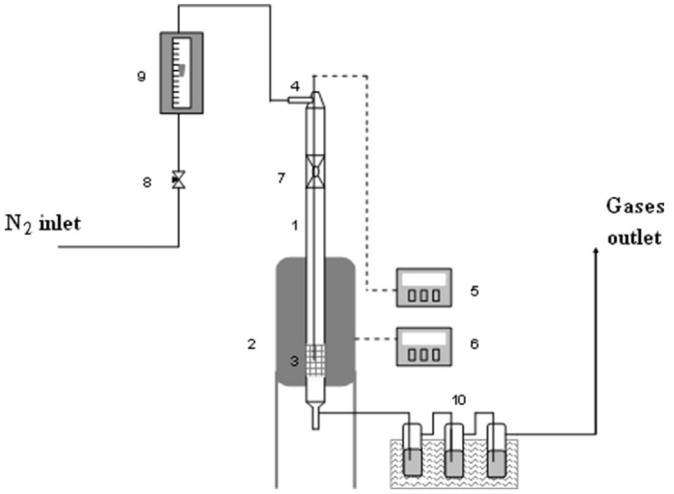

Fig. 1. Scheme of the equipment for pyrolysis assays 1) Reactor. 2) Electric furnace. 3) Sample carrier. 4) Thermocouple. 5) Reactor temperature indicator. 6) Furnace temperature controller/indicator. 7) Spherical valve. 8) Needle valve. 9) Rotameter. 10) Condensation system.

was separated from the latter by a valve. Nitrogen gas was supplied to purge oxygen and prevent further combustion of the sample. In order to start the pyrolysis process, the valve was opened and the sample carrier with an inserted chromel-alumel thermocouple was pushed and positioned in the reaction zone, which was heated by an electrical furnace. Thus, a heating rate of approximately 300 °C min^{-1} was achieved. At the reactor outlet, gaseous and liquid products circulated by a condensation system at − 10 °C which enabled condensation and collection of volatiles products. Furthermore, gaseous samples were collected at regular intervals employing gas sampling bags for further analysis. From preliminary experiments, the following pre-established operating conditions were chosen: T = 500 °C, N_2 flow rate = 300 mL min^{-1}, particle diameter = 250–500 μm; samples'masses = 10–15 g, holding time = 30 min.

The residual solid (bio-char and spent catalyst) and the accumulated liquid products contained in the flasks were weighed to determine product yields. These products were then carefully stored in closed containers for further characterization. Percent yields were calculated as weight of product per total weight of raw biomass sample (dry and catalyst-free). Gas yields were obtained by difference from overall mass balances.

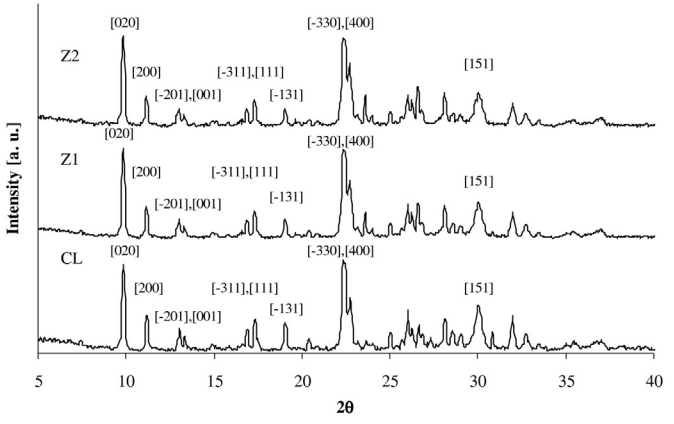

Fig. 2. Diffractograms for the natural clinoptilolite (CL) and the two developed catalysts (Z1 and Z2). Characteristic peaks of clinoptilolite are indicated.

2.6. Characterization of the pyrolysis products

Water content of the liquid samples was measured by volumetric Karl-Fischer titration (Metrohm Herisau Karl Fisher Automat E 547) following ASTM E 203. The samples' pH was determined with the same instrument depicted above (Section 2.3). Additionally, total phenol and sugar contents of the bio-oil were evaluated using the Folin-Ciocalteu and the phenol-sulphuric assays, respectively [28,29]. Dichloromethane

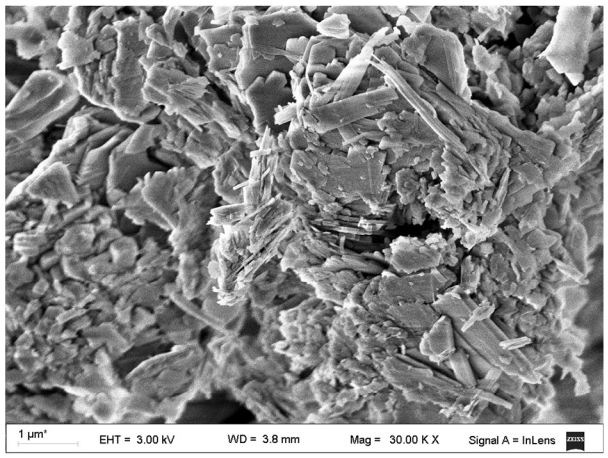

(a)

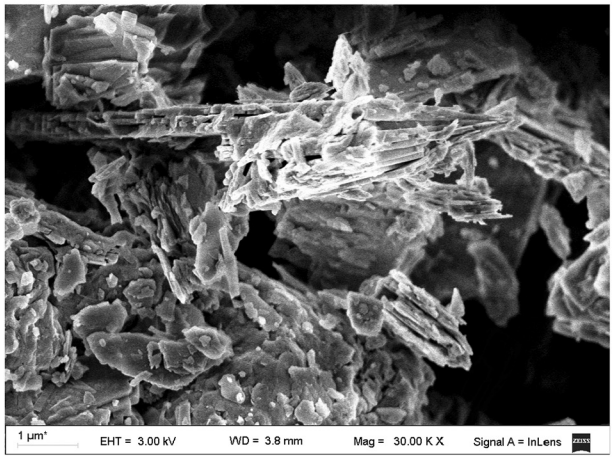

(b)

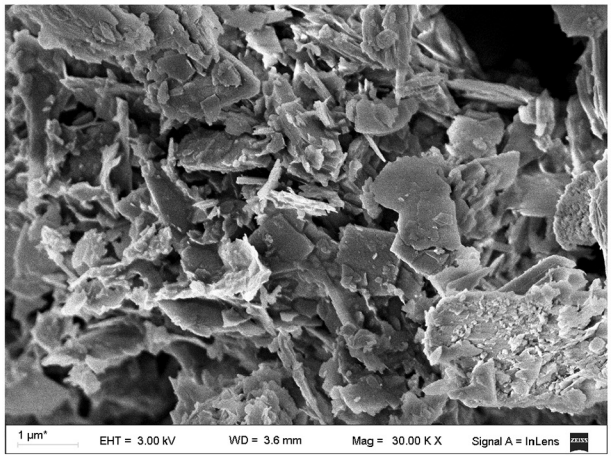

(c)

Fig. 3. SEM micrographs (30,000×) corresponding to the natural clinoptilolite (a), the alkaline catalyst Z1 (b) and the protonated catalyst Z2 (c).

Table 1
Surface concentration of the main present elements of clinoptilolite (CL) and the two developed catalysts (Z1 and Z2).

Surface concentration [wt%]	O	Na	Mg	Al	Si	K	Ca	Fe
CL	56.1	2.6	0.4	6.7	31.1	1.0	1.9	0.3
Z1	55.6	2.7	0.6	6.9	30.8	0.9	1.9	0.4
Z2	55.6	0.5	0.5	7.4	34.6	0.5	0.5	0.4

Table 2
Total acid sites (pyridine adsorption temperature = 100 °C) for the clinoptilolite (CL) and the developed catalysts (Z1 and Z2).

Sample	CL	Z1	Z2
Lewis [μmol g^{-1}]	12.9	9.9	8.1
Brønsted [μmol g^{-1}]	3.8	3.1	22.2

was used to extract the organic phase from the bio-oils (volume ratio solvent/bio-oil: 2:1) in order to determine their elemental composition by ultimate analyses, as depicted above. Furthermore, higher heating value (HHV) was also determined using a Parr 1341 oxygen bomb calorimeter.

Chemical compounds of bio-oils were identified using a Trace GC Ultra chromatograph coupled with a Thermo Scientific EM/DSQ II mass spectrometer (GC–MS). The employed capillary column was a Rxi-5 ms (length: 30 m; ID: 0.25 mm) and helium was used as carrier gas. Electron ionization (potential: 70 eV) was used and the measured mass range varied from 30 to 500 *m/z*.

Non-condensable gases, after flowing through the condensation system, were sampled periodically using Teflon gas bags, and further analyzed with a Shimadzu GC-8 gas chromatograph supplied with a thermal conductivity detector and a concentric packed Altech CTR I column (6 ft. × ¼ in.). Argon as carrier gas and a temperature of 25 °C were employed.

All the experiments were performed at least three times. Differences between replicates were less than 5% in all cases. Average values are reported.

3. Results and discussion

3.1. Characterization of the zeolite and the catalysts

Diffractograms of the clinoptilolite and the two derived catalysts are presented in Fig. 2. It can be seen that no important changes on the present phases arose from the treatments. Besides the clinoptilolite characteristic peaks, some impurities were present, such as quartz (21.0° and 26.7°) and other aluminosilicates, such as kaolinite and feldespate [30,31]. Fig. 3 shows the SEM micrographs of the clinoptilolite and the two catalysts developed from it. As it can be observed, materials are constituted by congregated plates of different dimensions. No noticeable morphological changes are appreciated as consequence of the thermal and/or ion exchange treatments.

Surface concentrations of the principal elements present in the samples, determined by SEM-EDS, are displayed in Table 1. Although most of the clinoptilolites are characterized by a greater proportion of K than Na, the studied zeolite showed an opposite trend. This may be due to a high Na content in the saline were the mineral was formed. Other authors have also reported the same trend for an Argentinean clinoptilolite [25]. On the other hand, the clinoptilolite presented an Al/Si molar relation of 0.224. As the natural clinoptilolite has an Al/Si molar relation of 0.2, the surface concentration analysis is in agreement with the small quantities of impurities detected by the X ray diffraction assays. It could be appreciated that the thermal treatment had no effect on the elements present on the material. In contrast, the ion exchange with NH_4^+ led to a reduction in Na^+, K^+ and Ca^{2+} in Z2 catalyst. These cations have a minor affinity with the zeolite frame than NH_4^+. Differently, the Mg^{2+} cation, which practically was not affected by ion exchange, would have a higher affinity with the clinoptilolite than NH_4^+ [32]. Likewise, the apparent increment on the surface concentrations of Al and Si for the Z2 catalyst may be attributed to the fact that most part of the alkaline and alkaline earth cations were replaced by NH_4^+, which was

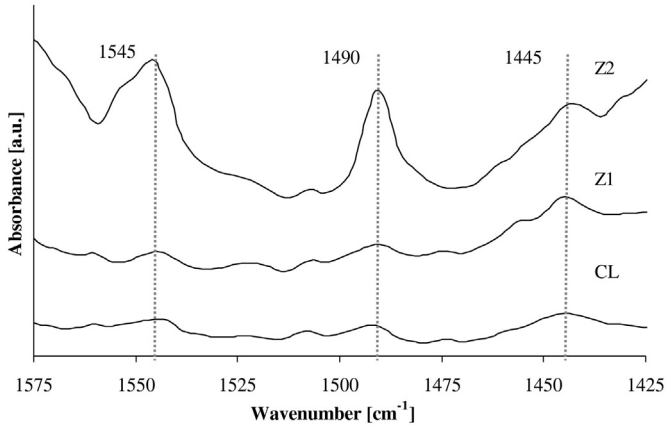

Fig. 4. FT-IR spectra for adsorbed pyridine at 100 °C for the clinoptilolite (CL) and the Z1 and Z2 catalysts.

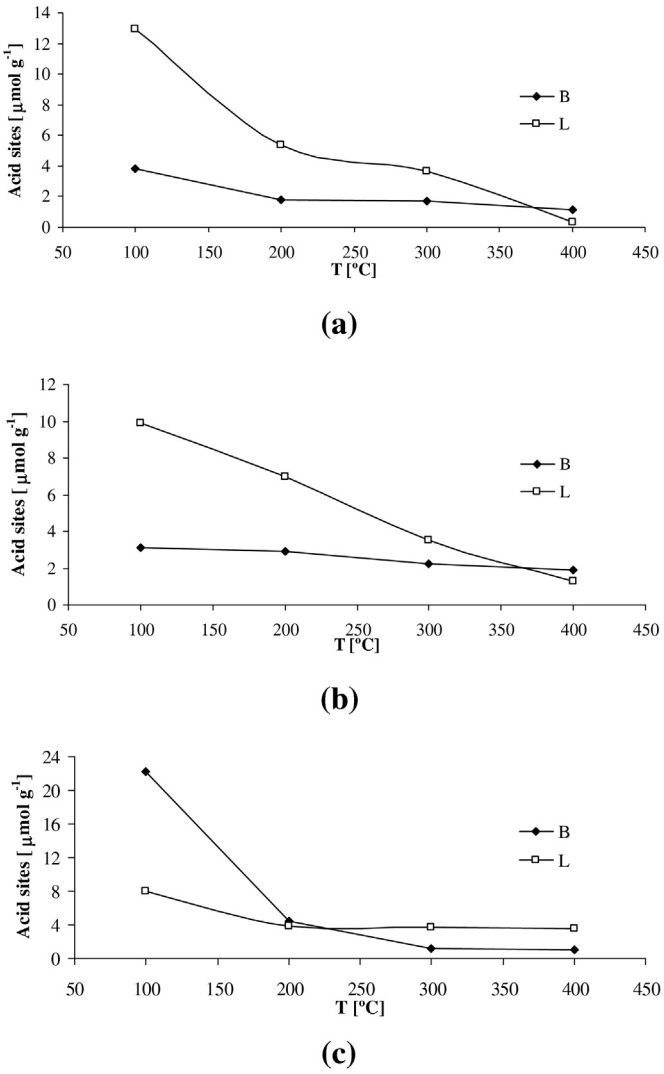

Fig. 5. Brønsted (B) and Lewis (L) acid sites for the clinoptilolite (a), the alkaline catalyst Z1 (b) and the protonated catalyst Z2 (c) at different desorption temperatures.

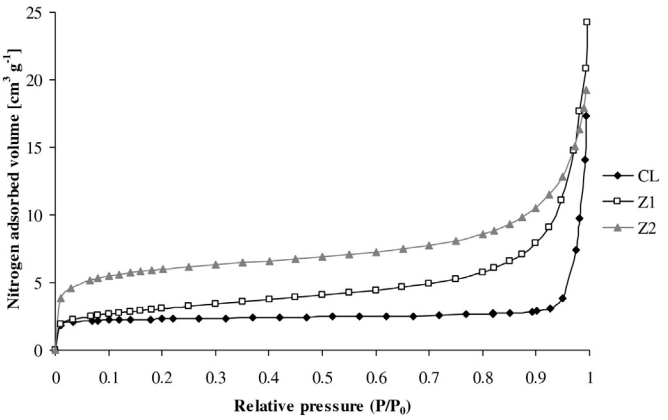

Fig. 6. Nitrogen adsorption isotherms (−196 °C) for the natural clinoptilolite (CL), the alkaline catalyst Z1, and the protonated catalyst Z2.

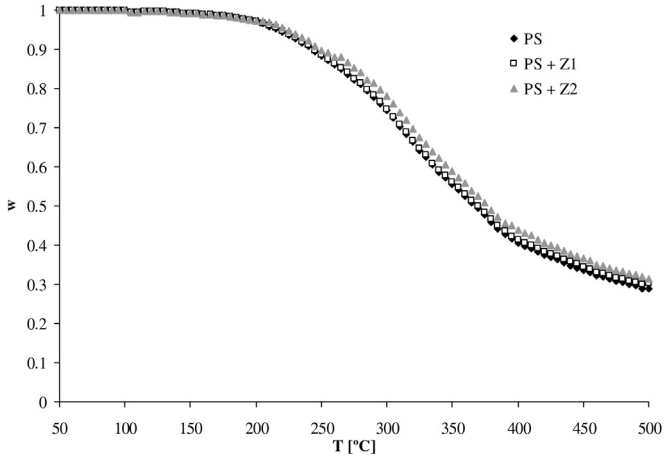

Fig. 7. TGA curves for the pyrolysis of peanut shells (PS) and of the shells in the presence of Z1 (PS + Z1) and Z2 (PS + Z2) catalysts. Biomass to catalyst ratio = 2:1.

subsequently decomposed to H^+ that is not detected by the EDS technique. As the surface concentrations are normalized according to the detected elements by the microscope probe, the contents of Al and Si rose. It has to be emphasized that no N was detected, suggesting that a complete conversion of NH_4^+ to H^+ was achieved.

FT-IR spectra (absorbance) of adsorbed pyridine on the clinoptilolite and the Z1 and Z2 catalysts are exhibited in Fig. 4. Three different peaks at wavenumbers of 1545, 1490 and 1445 cm^{-1} may be identified. The first one would correspond to pyridinium ions (Brønsted sites), whereas the last band is usually assigned to molecular pyridine (Lewis sites). The band whose wavenumber is 1490 cm^{-1} is due to both types of adsorption. The areas below the peaks at 1545 cm^{-1} and 1445 cm^{-1} were integrated and used to calculate acid site concentration according to Eq. (1). These values are presented in Table 2. The total amount of acid sites for the natural clinoptilolite is comparable to values informed in the literature [21]. Clearly, the ion exchange treatment followed by calcination generated a great amount of Brønsted acid sites on the Z2 catalyst. However, the sole calcination of the zeolite had not an important influence on the acid sites, as seen in the similar values for CL and Z1. These results were consistent with the measured pH for the three materials. While the pH for CL and Z1 was of 6.0 and 8.0, respectively, the value for Z2 was 4.3.

Likewise, the strength of the acid sites was examined from the assays of pyridine adsorption at different temperatures. The results are shown in Fig. 5. It is worth mentioning that even though Z2 had a larger amount of Brønsted acid sites, a significant proportion of them did not retain pyridine at temperatures of 200 °C or higher. Despite the fact that the temperature of the pyrolysis experiments (500 °C) was much higher indicating that the volatiles would preferentially react with the Lewis sites, it should be noted that the characterizations of acid sites shown in Fig. 5 were obtained after equilibrium was established. In the pyrolysis assays, the short residence time did not allow the equilibrium to be reached and as the Brønsted sites are more reactive than those of Lewis, the pyrolysis vapours would preferentially react with the former ones [26].

Nitrogen adsorption isotherms for the clinoptilolite and the two catalysts are illustrated in Fig. 6. It could be seen that the shape of the isotherms corresponding to the samples presented typical characteristics of isotherms between type I and type II according to IUPAC classification [33]. Textural properties evaluated from the isotherms are listed in Table 3. The results indicate that both treatments applied increased the BET area, particularly for Z2. Furthermore, R_m decreased notably for this catalyst, implying that more micropores were created in the treatment applied. The size and shape of the pores are very important characteristics in connection with the accessibility of the vapours to reach the acid sites, and the occurrence of the catalytic cracking [34].

Table 3
Textural properties of the clinoptilolite (CL) and the catalysts (Z1 and Z2).

Sample	CL	Z1	Z2
S_{BET} [m^2 g^{-1}]	6.3	10.3	19.7
V_t [cm^3 g^{-1}]	0.02	0.03	0.03
R_m [nm]	6.4	5.8	2.6

3.2. Thermal behavior of the peanut shells

The effect of the presence of the catalysts on the pyrolysis behavior of the peanut shells was examined. Fig. 7 illustrates variations of the weight fractions (w) with the temperature. The weight fractions were obtained as $w = m/m_0$, where m and m_0 are the dry mass of the sample (catalyst-free) at time t and the initial dry mass, respectively. Thermal degradation of PS exhibits a sigmoidal degradation pattern. Decrease of w up to temperatures of 400 °C may be mainly attributed to holocellulose degradation while the drop of w at higher temperatures would be due to lignin decomposition [35]. As observed in Fig. 7, the presence of the catalysts does not almost modify the thermal degradation of the biomass. This fact suggests that the catalyst would only affect the secondary reactions that would occur after the primary volatilization, leading to vapor reforming and subsequent bio-oil generation. Small differences among the instant mass fractions have been attributed to coke deposition on the catalyst surface [16].

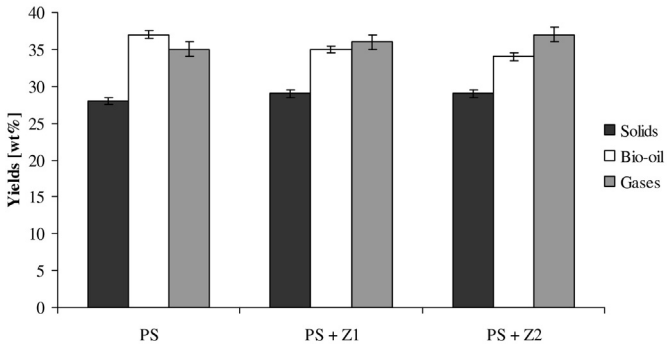

Fig. 8. Product yields for the pyrolysis of the peanut shells (PS) and of the shells in the presence of the alkaline (PS + Z1) and the protonated catalysts (PS + Z2). Biomass to catalyst ratio = 2:1; temperature = 500 °C.

Table 4
Elemental composition and high heating value of the bio-oils generated by the conventional pyrolysis (PS) and the *in-situ* catalytic process (PS + Z1 and PS + Z2).

Bio-oil	PS	PS + Z1	PS + Z2
Ultimate Analysis [wt%]			
Carbon	49.3	56.4	59.1
Hydrogen	8.1	7.5	7.0
Nitrogen	2.9	1.7	1.1
Oxygen[a]	39.7	34.4	32.8
HHV [MJ kg^{-1}]	22.5	24.9	25.5

[a] Estimated by difference.

3.3. Yields of the pyrolysis products

Yields of the three kinds of pyrolysis products for the thermal degradation of the lignocelullosic biomass individually and in the presence of each catalyst at 500 °C are presented in Fig. 8. Almost no differences were found for the solid yields for the three studied alternatives. Very small differences could be due to coke deposition on the catalyst surface. Since in the present experiments little coke (less than 4 wt% of the spent catalyst as determined by TGA analysis in an oxidizing atmosphere) as deposited on the catalyst, it might be inferred that the cracking was mild. These results are in accordance with the trend observed for the influence of the catalysts on the residual weight fractions (w at T = 500 °C) of the TGA curves shown in Fig. 7.

The catalytic pyrolysis of PS with both catalysts led to a diminution of the bio-oil production and an increase of the gas generation, particularly for Z2 catalyst. This could be explained taking into account that oxygen removal from the bio-oil by catalytic cracking generated more CO and CO_2 that are added to the ones produced by the primary degradation of the biomass. According to Corma et al. [36], deoxygenation of bio-oil by catalytic cracking could be represented by the following general chemical equation:

$$C_6H_{12}O_6 \rightarrow aC_xH_{2x+2}O_y + bCO_2 + cCO + dH_2O + eC \quad (3)$$

Therefore, besides the improved bio-oil, CO, CO_2, water and coke are also generated.

3.4. Properties of the pyrolysis products

Since no differences were detected among the elemental compositions of the bio-char generated by conventional pyrolysis and of those produced by catalytic pyrolysis, in this subsection only the characteristics of the bio-oils and gases are discussed. Table 4 lists the results of the elemental analysis and HHV of the bio-oils produced by the conventional and catalytic pyrolysis at 500 °C. The elemental composition of the biomass (Section 2.1) and the bio-oil arising from the conventional pyrolysis of the shells were very similar. By contrast, biomass pyrolysis in presence of the two catalysts led to a bio-oil with less oxygen and enriched in carbon. This also contributed to a higher HHV of the biofuels, particularly when Z2 catalyst was used.

Table 5 presents the contents of water, total phenol and sugars and pH values of the different bio-oils. Both catalytic processes led to bio-oils with a higher amount of water, particularly for Z1, than the conventional process, as expected from Eq. (3). pH values of the bio-oils were low (around 3) mainly due to high concentrations of acetic and formic acids [8]. Concerning phenols generation, both catalysts induced a higher production of this type of compounds, in agreement with other reported results [21]. Ma et al. [37] suggested that the phenolic fragments arising from pyrolysis of lignin, in presence of mesoporous materials, become more stable and do not repolymerize to form coke. Thus, after condensation, they form part of the bio-oil. Moreover, the *in-situ* catalytic pyrolysis considerably reduced the sugar content in the bio-oils. Mihalcik et al. [15] reported an important reduction on levoglucosan generation from pyrolysis of oak, maize husk and switchgrass when several zeolites were utilized (HSMZ-5, H-Y, H-β and H-mordenite).

Table 5
Water content, total phenol and sugar contents, and pH for the bio-oils generated by the conventional pyrolysis (PS) and the *in-situ* catalytic process (PS + Z1 and PS + Z2).

Bio-oil	PS	PS + Z1	PS + Z2
Water [wt%]	51.3	57.0	54.8
Phenols [g dm^{-3}][a]	16.4	18.2	21.9
Sugar [g dm^{-3}][a]	6.2	1.3	1.5
pH	3.1	3.0	3.2

[a] Aqueous phase.

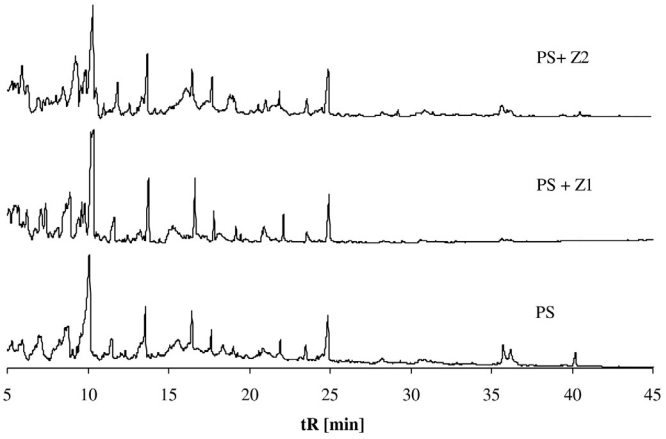

Fig. 9. Total ion chromatograms of the bio-oils produced by the conventional pyrolysis of the peanut shells (PS) and by the catalytic pyrolysis (PS + Z1 and PS + Z2).

Total ion chromatograms of the bio-oils produced by conventional and *in-situ* catalytic pyrolysis using both catalysts are displayed in Fig. 9. Retention times (RT) below 5 min are not shown as the solvent front was found for these values. Main compounds are listed in Table 6. They were identified by means of residence times and mass spectra found in the literature [38–40]. The main difference in the chromatograms was the reduction of the peak assigned to the levoglucosan and its isomer, 1-6-anhydro-β-D-glucofuranose, for the bio-oils produced by the catalytic process. These results were in concordance with the lower values of sugar concentration when the phenol-sulfuric assay was carried out.

The yields of the main gases of pyrolysis, calculated on the basis of moles of generated gas per kg of pyrolyzed sample are displayed in Fig. 10. The results show that when pyrolyzed individually, PS led to a greater CO generation than that of CO_2. On the other hand, when the pyrolysis was performed in the presence of the catalysts the trend was reversed. The higher oxygen content in the gases was in agreement with

Table 6
Main compounds detected in bio-oils by GC/MS analysis.

RT [min]	Compound
6.7	Phenol
8.1	2-Hydroxy-3-methyl-2-cyclopenten-1-one
8.8	p-Cresol
9.7	2-Methoxyphenol (guaiacol)
10.9	5-Hydroxymethylfurfural
13.5	2-Methoxy-4-methylphenol (creosol)
15.0	Catechol
18.6	2,6-Dimethoxyphenol (syringol)
20.5	Vanillin
21.6	2-Methoxy-4-propenylphenol (eugenol)
24.4	2-Methoxy-4-propylphenol
35.0	2,6-Dimethoxy-4-propylphenol
35.6	Levoglucosan
40.1	1,6-β-D-Glucofuranose

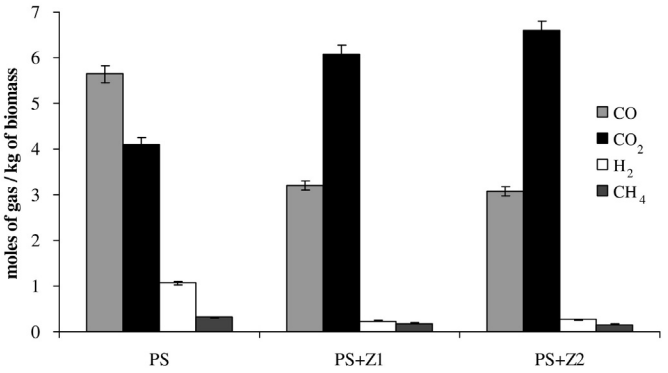

Fig. 10. Generation of the main gases arising from conventional (PS) and catalytic pyrolysis of the peanut shells (PS + Z1 and PS + Z2).

the lower oxygen content of the bio-oils. In addition, the generation of CH_4 and H_2 decreased if catalysts were present. Since the catalysts would stabilize the phenolic fragments derived from the lignin of the shells, and the thermal degradation of this biopolymer is the main responsible of CH_4 and H_2 generation, the catalytic pyrolysis of the shells would result in a lower production of these two gases [37,41]. The HHV of the gaseous products [MJ kg biomass^{-1}] was calculated as the sum of the product of the moles of each gas generated per kg of biomass sample (G_i) and the heat of combustion of each gas [MJ mol^{-1}]:

$$HHV = 0.802G_{CH_4} + 0.286G_{H_2} + 0.283G_{CO} \quad (4)$$

The HHV for the pyrolysis gases arising from PS was 1.9 MJ kg biomass^{-1}, while when Z1 and Z2 catalysts were employed values of 1.2 and 1.1 MJ kg biomass^{-1} were obtained, respectively. Lower values were due to the lower concentrations of CO, CH_4 and H_2 generated in catalytic pyrolysis.

4. Conclusions

In-situ catalytic pyrolysis of peanut shells employing two different catalysts based on clinoptilolite led to a reduction in bio-oil oxygen content, which would increase its stability and miscibility with conventional fuels. Regarding their efficiency, the protonated catalyst performed better as not only gave rise to a more deoxygenated bio-oil but also generated less water. Moreover, in comparison with the alkaline catalyst, it produced more CO_2 as by-product. This fact suggests that the selectivity of reactions which generate these undesirable by-products, water and CO_2, would be susceptible of the type of acid sites present on the catalyst. As CO_2 separation from the bio-oil is simpler than water elimination and since CO_2 does not contribute to lower bio-oil heating value, the employment of the protonated catalyst emerges as a better choice to produce a higher quality bio-oil by *in-situ* catalytic pyrolysis of peanut shells.

Acknowledgements

The authors gratefully acknowledge Agencia Nacional de Promoción Científica y Tecnológica (ANPCYT–FONCYT PICT 2012–2188), Consejo Nacional de Investigaciones Científicas y Técnicas (CONICET PIP 0183), and Universidad de Buenos Aires (UBA 20020130100605BA) from Argentina, for financial support.

References

[1] FAOSTAT, Browse Data, Publication, Crops. Food and Agriculture Organization of the United Nations, http://faostat3.fao.org/browse/Q/QC/E2016 (accessed 16.06.16).
[2] P. Arromdee, V.I. Kuprianov, Combustion of peanut shells in a cone-shaped bubbling fluidized-bed combustor using alumina as the bed material, Appl. Energy 97 (2012) 470–482.
[3] X. Liu, X.T. Bi, Removal of inorganic constituents from pine barks and switchgrass, Fuel Process. Technol. 92 (2011) 1273–1279.
[4] R. Saidur, E.A. Abdelaziz, A. Demirbas, M.S. Hossain, S. Mekhilef, A review on biomass as a fuel for boilers, Renew. Sust. Energ. Rev. 15 (2011) 2262–2289.
[5] V. Menon, M. Rao, Trends in bioconversion of lignocellulose: biofuels, platform chemicals & biorefinery concept, Prog. Energy Combust. Sci. 38 (2012) 522–550.
[6] A. Demirbas, Political, economic and environmental impacts of biofuels: a review, Appl. Energy 86 (2009) S108–S117.
[7] A.L. Cukierman, G.V. Nunell, M.E. Fernandez, J. De Celis, M.R. Kim, L. Gurevich Messina, P.R. Bonelli, Thermochemical processing of wood from invasive arboreal species for sustainable bioenergy generation and activated carbons production, in: J.J. Blanco, A.T. Fernandes (Eds.), Invasive Species: Threats, Ecological Impact and Control Methods, Nova Publishers Inc., New York 2012, pp. 1–45.
[8] A.V. Bridgwater, Review of fast pyrolysis of biomass and product upgrading, Biomass Bioenergy 38 (2012) 68–94.
[9] L. Zhang, C. Xu, P. Champagne, Overview of recent advances in thermo-chemical conversion of biomass, Energy Convers. Manag. 51 (2010) 969–982.
[10] K. Jacobson, K.C. Maheria, A. Kumar Dalai, Bio-oil valorization: a review, Renew. Sust. Energ. Rev. 23 (2013) 91–106.
[11] D. Chiaramonti, A. Oasmaa, Y. Solantausta, Power generation using fast pyrolysis liquids from biomass, Renew. Sust. Energ. Rev. 11 (2007) 1056–1086.
[12] J. Lehto, A. Oasmaa, Y. Solantausta, M. Kytö, D. Chiaramonti, Review of fuel oil quality and combustion of fast pyrolysis bio-oils from lignocellulosic biomass, Appl. Energy 116 (2014) 178–190.
[13] T.P. Vispute, H. Zhang, A. Sanna, R. Xiao, G.W. Huber, Renewable chemical commodity feedstocks from integrated catalytic processing of pyrolysis oils, Science 330 (2010) 1222–1227.
[14] P.M. Mortensen, J.-D. Grunwaldt, P.A. Jensen, K.G. Knudsen, A.D. Jensen, A review of catalytic upgrading of bio-oil to engine fuels, Appl. Catal. A Gen. 407 (2011) 1–19.
[15] D.J. Mihalcik, C.A. Mullen, A.A. Boateng, Screening acidic zeolites for catalytic fast pyrolysis of biomass and its components, J. Anal. Appl. Pyrolysis 92 (2011) 224–232.
[16] A. Aho, N. DeMartini, A. Pranovich, J. Krogell, N. Kumar, K. Eränen, B. Holmbom, T. Salmi, M. Hupa, D.Y. Murzin, Pyrolysis of pine and gasification of pine chars–influence of organically bound metals, Bioresour. Technol. 128 (2013) 22–29.
[17] K. Wang, P.A. Johnston, R.C. Brown, Comparison of in-situ and ex-situ catalytic pyrolysis in a micro-reactor system, Bioresour. Technol. 173 (2015) 124–131.
[18] J.D. Adjaye, S.P.R. Katikaneni, N.N. Bakhshi, Catalytic conversion of a biofuel to hydrocarbons: effect of mixtures of HZSM-5 and silica-alumina catalysts on product distribution, Fuel Process. Technol. 48 (1996) 115–143.
[19] C. Perego, R. Bagatin, M. Tagliabue, R. Vignola, Zeolites and related mesoporous materials for multi-talented environmental solutions, Microporous Mesoporous Mater. 166 (2013) 37–49.
[20] E. Pütün, B.B. Uzun, A.E. Pütün, Rapid pyrolysis of olive residue. 2. Effect of catalytic upgrading of pyrolysis vapors in a two-stage fixed-bed reactor, Energy Fuels (2009) 2248–2258.
[21] N. Rajić, N.Z. Logar, A. Rečnik, M. El-Roz, F. Thibault-Starzyk, P. Sprenger, L. Hannevold, A. Andersen, M. Stöcker, Hardwood lignin pyrolysis in the presence of nano-oxide particles embedded onto natural clinoptilolite, Microporous Mesoporous Mater. 176 (2013) 162–167.
[22] J. Milovanović, N. Rajić, R.E. Stensrød, E.M. Myhrvold, R. Tschentscher, M. Stöcker, Lignin pyrolysis in the presence of oxide particles embedded onto natural clinoptilolite and ZSM-5, Conference Paper, September 2014 Conference: 6th FEZA Conference, at Leipzig, Germany.
[23] J. Milovanović, R. Stensrød, E. Myhrvold, R. Tschentscher, M. Stöcker, S. Lazarevic, N. Rajić, Modification of natural clinoptilolite and ZSM-5 with different oxides and studying of the obtained products in lignin pyrolysis, J. Serbian Chem. Soc. 80 (2015) 717–729.
[24] A. Aho, N. Kumar, K. Eränen, T. Salmi, M. Hupa, D.Y. Murzin, Catalytic pyrolysis of woody biomass in a fluidized bed reactor: influence of the zeolite structure, Fuel 87 (2008) 2493–2501.
[25] I.L. Botto, M.E. Canafoglia, I.D. Lick, C.I. Cabello, I.B. Schalamuk, G. Minelli, G. Ferraris, Environmental application of natural microporous aluminosilicates: NOx reduction by propane over modified clinoptilolite zeolite, J. Arg. Chem. Soc. 92 (2004) 139–153.
[26] C.A. Emeis, Determination of integrated molar extinction coefficients for infrared absorption bands of pyridine adsorbed on solid acid catalysts, J. Catal. 141 (1993) 347–354.
[27] M.E. Fernandez, G.V. Nunell, P.R. Bonelli, A.L. Cukierman, Activated carbon developed from orange peels: batch and dynamic competitive adsorption of basic dyes, Ind. Crop. Prod. 62 (2014) 437–445.
[28] M.R. Rover, R.C. Brown, Quantification of total phenols in bio-oil using the Folin–Ciocalteu method, J. Anal. Appl. Pyrolysis 104 (2013) 366–371.
[29] M.R. Rover, P.A. Johnston, B.P. Lamsal, R.C. Brown, Total water-soluble sugars quantification in bio-oil using the phenol–sulfuric acid assay, J. Anal. Appl. Pyrolysis 104 (2013) 194–201.
[30] S. Yaşyerli, I. Ar, G. Doğu, T. Doğu, Removal of hydrogen sulfide by clinoptilolite in a fixed bed adsorber, Chem. Eng. Process. 41 (2002) 785–792.
[31] Y.F. Tao, Y. Qiu, S.Y. Fang, Z.Y. Liu, Y. Wang, J.H. Zhu, Trapping the lead ion in multi-components aqueous solution by natural clinoptilolite, J. Hazard. Mater. 180 (2010) 282–288.
[32] T. Ünaldı, İ. Mızrak, S. Kadir, Physicochemical characterisation of natural K-clinoptilolite and heavy-metal forms from Gördes (Manisa, western Turkey), J. Mol. Struct. 1054-1055 (2013) 349–358.
[33] F. Rouquerol, J. Rouquerol, K. Sing, Adsorption by Powders and Porous Solids. Principles, Methodology and Applications, Academic Press, 1999.

[34] M. Stöcker, Gas phase catalysis by zeolites, Microporous Mesoporous Mater. 82 (2005) 257–292.
[35] J.D. González, M.R. Kim, E.L. Buonomo, P.R. Bonelli, A.L. Cukierman, Pyrolysis of biomass from sustainable energy plantations: effect of mineral matter reduction on kinetics and charcoal pore structure, Energy Sources, Part A: Recover, Util. Environ. Effects 30 (2008) 809–817.
[36] A. Corma, G. Huber, L. Sauvanaud, P. Oconnor, Processing biomass-derived oxygenates in the oil refinery: catalytic cracking (FCC) reaction pathways and role of catalyst, J. Catal. 247 (2007) 307–327.
[37] Z. Ma, E. Troussard, J.A. Van Bokhoven, Controlling the selectivity to chemicals from lignin via catalytic fast pyrolysis, Appl. Catal. A Gen. 423-424 (2012) 130–136.
[38] P. Patwardhan, J.A. Satrio, R.C. Brown, B.H. Shanks, Product distribution from fast pyrolysis of glucose-based carbohydrates, J. Anal. Appl. Pyrolysis 86 (2009) 323–330.
[39] T. Ohra-aho, J. Linnekoski, Catalytic pyrolysis of lignin by using analytical pyrolysis-GC–MS, J. Anal. Appl. Pyrolysis 113 (2015) 186–192.
[40] NIST Chemistry WebBook, NIST Standard Reference Database Number 69, National Institute of Standards and Technology, http://webbook.nist.gov/chemistry2016 (accessed 16.06.16).
[41] F.-X. Collard, J. Blin, A review on pyrolysis of biomass constituents: mechanisms and composition of the products obtained from the conversion of cellulose, hemicelluloses and lignin, Renew. Sust. Energ. Rev. 38 (2014) 594–608.